

# The effect of Al<sub>2</sub>O<sub>3</sub>-coating coverage on the electrochemical properties in LiCoO<sub>2</sub> thin films

Yuhong Oh · Donggi Ahn · Seunghoon Nam ·  
Byungwoo Park

Received: 5 August 2009 / Revised: 28 September 2009 / Accepted: 2 October 2009 / Published online: 23 October 2009  
© Springer-Verlag 2009

**Abstract** The electrochemical properties of nanoscale Al<sub>2</sub>O<sub>3</sub>-coated LiCoO<sub>2</sub> thin films were examined as a function of the coating coverage. Al<sub>2</sub>O<sub>3</sub>-coated LiCoO<sub>2</sub> films showed enhanced cycle-life performance with increasing degree of coating coverage, which was attributed to the suppression of Co dissolution and F<sup>-</sup> concentration in the electrolyte. Moreover, an Al<sub>2</sub>O<sub>3</sub>-coating layer with partial coverage clearly improved the electrochemical properties, even at 60 °C or with a water-contaminated electrolyte. Even though metal-oxide coating on LiCoO<sub>2</sub> has been actively investigated, the mechanisms of nanoscale coating have yet to be clearly identified. In this article, surface analysis suggested that the Al<sub>2</sub>O<sub>3</sub>-coating layer had transformed to an AlF<sub>3</sub>·3H<sub>2</sub>O layer during cycling, which inhibited the generation of HF by scavenging H<sub>2</sub>O molecules present in the electrolyte.

**Keywords** Li-ion battery · LiCoO<sub>2</sub> · Al<sub>2</sub>O<sub>3</sub> ·  
Nanoscale coating · H<sub>2</sub>O scavenge

## Introduction

Recently, hexagonal LiCoO<sub>2</sub> cathode materials have been used in most commercial lithium-ion batteries on account of their simple preparation, high specific capacity, and good electrochemical properties [1]. However, Li<sub>x</sub>CoO<sub>2</sub> is typi-

cally charged up to ~4.2 V vs. Li (Li<sub>0.5</sub>CoO<sub>2</sub>), yielding a specific capacity below ~140 mAh/g. Further increased charge cutoff voltage results in significant deteriorations of LiCoO<sub>2</sub>. This is attributed to structural changes in the unit-cell volume [2], increased cobalt dissolution into the organic electrolyte [3], loss of oxygen [4], formation of electrochemically resistive surface films [5], etc.

An effective method of resolving the problem of capacity fading at high cutoff voltage is thermal treatment [6, 7] or coating the surface of cathode with various materials (metal oxide, metal phosphate, or other materials) [8–22]. It was previously reported that a nanoscale metal-oxide coating on the surface of cathode improved the electrochemical properties at high cutoff voltages and current rates [8–13, 17–21]. Thackeray et al. reported enhanced capacity and stability in cycling by coating ZrO<sub>2</sub> on LiMn<sub>2</sub>O<sub>4</sub>, and speculated that the enhanced performance of spinel was attributed to its ability of ZrO<sub>2</sub> particles to neutralize the HF component from the electrolyte [23]. Myung et al. also reported that a metal-oxide coating layer on Li<sub>1.05</sub>Ni<sub>0.4</sub>Co<sub>0.15</sub>Mn<sub>0.4</sub>O<sub>2</sub> acted as an HF scavenger, and they suggested the following reaction: Al<sub>2</sub>O<sub>3</sub>+6HF→2AlF<sub>3</sub>+3H<sub>2</sub>O [24, 25]. However, H<sub>2</sub>O generated from the reaction between Al<sub>2</sub>O<sub>3</sub> and HF regenerates HF in the electrolyte, and the same things happen again consequently. My group reported that metal-oxide coating on LiCoO<sub>2</sub> can affect lattice expansion during cycling [8, 9]. Some other researchers suggested that a partial or non-uniform coating still improved the electrochemical properties of powder materials [26, 27]. My group recently reported that Al<sub>2</sub>O<sub>3</sub>-coated LiCoO<sub>2</sub> thin film with even 50% coating coverage showed enhanced cycle-life performance with no evidence of mechanisms [28], and Al<sub>2</sub>O<sub>3</sub> coating on LiCoO<sub>2</sub> powder was also carefully investigated by Fey et al. [29, 30]. These results were correlated with the

Yuhong Oh and Donggi Ahn contributed equally to this work.

Y. Oh · D. Ahn · S. Nam · B. Park (✉)  
Department of Materials Science and Engineering,  
and Research Center for Energy Conversion and Storage,  
Seoul National University,  
Seoul 151-744, Korea  
e-mail: byungwoo@snu.ac.kr

suppression of Co dissolution during electrochemical cycling. However, the mechanisms of metal-oxide coating have yet to be clearly identified.

Characterizing the intrinsic properties of LiCoO<sub>2</sub> powders is complicated, because the powder geometry consists of polymer binders and carbon blacks for the required electronic conduction among the ~10 μm powders. Therefore, thin-film geometry is appropriate for investigating the intrinsic properties of nanoscale coating on LiCoO<sub>2</sub>, because it has only a cathode and metal-oxide electrolyte interface, and is insensitive to the coating thickness on cycle-life performance [10]. In this article, thin-film LiCoO<sub>2</sub> cathodes were examined by distinctly controlling the coating coverage, cycling temperature, and level of water contamination in order to clarify the scavenge mechanisms.

## Experimental section

LiCoO<sub>2</sub> thin films were deposited on thermally oxidized Si (100) substrates using RF magnetron sputtering of a LiCoO<sub>2</sub> target. A Pt current collector was deposited onto a TiO<sub>2</sub> adhesion layer, and the LiCoO<sub>2</sub> film was deposited on the Pt layer. An approximately 600-nm-thick LiCoO<sub>2</sub> was deposited at a pressure of 20 mTorr with an Ar/O<sub>2</sub> ratio of 3/1 after presputtering for 1 h. To obtain high-quality LiCoO<sub>2</sub>, all films were annealed at 700 °C in an oxygen atmosphere at 20 mTorr for 30 min. The 10-nm-thick Al<sub>2</sub>O<sub>3</sub> thin films with a coating coverage ranging from 25% to 100% were deposited on top of the crystallized LiCoO<sub>2</sub> films by reactive sputtering of an Al target. The Al<sub>2</sub>O<sub>3</sub>-coating patterns with 75%, 50%, and 25% coverage consisted of 1,000, 360, and 150 μm squares, respectively, with a distance of 150 μm between the nearest squares. After Al<sub>2</sub>O<sub>3</sub> deposition, the coated and bare samples were heat-treated at 400 °C for 2 h in an oxygen atmosphere.

Beaker-type half cells were used to evaluate the electrochemical properties. The cells were made up of Li-metal sheets as a counter and reference electrode, a LiCoO<sub>2</sub> cathode with an active area of ~1 cm<sup>2</sup> as a working electrode, and 1 M LiPF<sub>6</sub> in ethylene carbonate/diethyl carbonate (EC/DEC, 1/1 vol.%, water impurities of less than 20 ppm) (Cheil Industries, Inc.) as the electrolyte. The cells were electrochemically cycled over the voltage range of 2.75 and 4.4 V by applying a current density of 0.4 mA/cm<sup>2</sup> (= 12 C) at 25 °C and 60 °C. At all the charge/discharge cutoff steps, the cell voltages were potentiostated until the current decreased to 10% of the charge/discharge rate with a time limit of 10 min. The charge-transfer resistance of cathodes with the bare and coated LiCoO<sub>2</sub> films was measured by electrochemical impedance spectroscopy (EIS) from 10 mHz to 100 kHz with an ac signal amplitude of 5 mV. The EIS

was measured at a 4.2 V charged state with a current less than 1 μA/cm<sup>2</sup>, during the initial cycle, and after the tenth, 40th, and 80th cycles.

Inductively coupled plasma–mass spectroscopy was used to measure the extent of cobalt dissolution into the electrolyte, after floating the 4.6 V charged cathodes for 12 days at 25 °C. The fluorine-ion concentration in the electrolyte was measured by ion chromatography (IC, Dionex 500). The effects of water impurities on the electrochemical properties of LiCoO<sub>2</sub> were examined by cycling the cells at 25 °C with a 200 ppm water-contaminated electrolyte. The compounds on the surface of cathode materials were examined using a time-of-flight secondary-ion mass spectroscopy (ToF-SIMS, PHI7200) surface analyzer equipped with a 7.9 keV Cs ion source and pulse-electron flooding.

## Results and discussion

The electrochemical performance was examined by cycling the Al<sub>2</sub>O<sub>3</sub>-coated LiCoO<sub>2</sub> thin films with a surface coverage ranging from 0% to 100%. Figure 1 shows the cycle-life performance of the bare and Al<sub>2</sub>O<sub>3</sub>-coated LiCoO<sub>2</sub> films, excluding the capacity at constant-voltage mode. The Al<sub>2</sub>O<sub>3</sub>-coated LiCoO<sub>2</sub> films show improved capacity retention with increasing coating coverage. Non-linearity of charge and discharge capacities above 70 cycles is attributed to the slower kinetics of Li<sup>+</sup> de-intercalation in

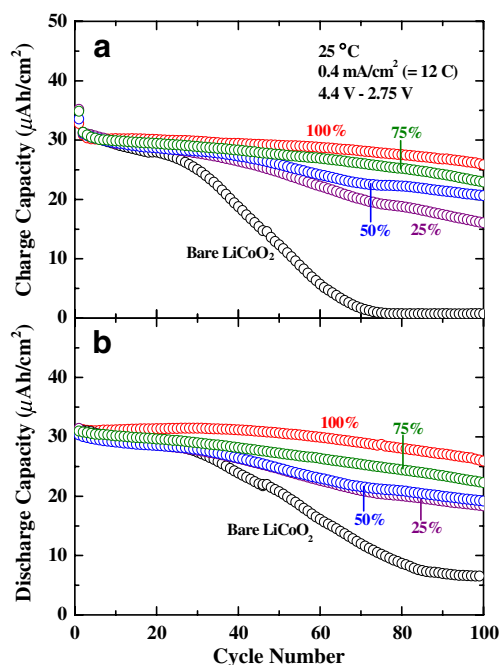


**Fig. 1** **a** The charge- and **b** discharge capacity retention of bare and Al<sub>2</sub>O<sub>3</sub>-coated LiCoO<sub>2</sub> thin films (charged to 4.4 V at 12 C) as a function of coating coverage ranging from 25% to 100%

bare LiCoO<sub>2</sub> than Li<sup>+</sup> intercalation, as observed by a galvanostatic intermittent titration technique, since the extra capacity from the constant-voltage mode (at 4.4 and 2.75 V) is not included [10, 15].

The voltage profiles of the bare and Al<sub>2</sub>O<sub>3</sub>-coated LiCoO<sub>2</sub> thin films with various degrees of surface coverage (observed at 25 °C) are shown in Fig. 2. Compared with the profiles of the bare LiCoO<sub>2</sub>, a slight increase in polarization is observed in the initial cycle of the Al<sub>2</sub>O<sub>3</sub>-coated cathodes. From the second cycle, the polarization in the charge and discharge processes of the coated sample becomes less significant [10, 15].

In order to correlate the cycle-life performance of thin-film LiCoO<sub>2</sub> with the electrode kinetics, EIS analysis of both the bare and Al<sub>2</sub>O<sub>3</sub>-coated LiCoO<sub>2</sub> films with different degrees of surface coverage was carried out after cycling, as shown in Fig. 3. Before the EIS measurements, all cells were cycled at 0.4 mA/cm<sup>2</sup> between 4.4 and 2.75 V, and potentiostated at 4.2 V until the current density had decreased to 1 μA/cm<sup>2</sup>. All the LiCoO<sub>2</sub> thin films during the first cycle show similar charge-transfer resistance (*R*<sub>ct</sub>), indicating that *R*<sub>ct</sub> at the interface of the Al<sub>2</sub>O<sub>3</sub>-coating layer and LiCoO<sub>2</sub> film is comparable to that of the electrolyte and LiCoO<sub>2</sub> film during the initial cycle. However, *R*<sub>ct</sub> of the bare LiCoO<sub>2</sub> significantly increases with increasing number of cycles compared with the coated LiCoO<sub>2</sub> films. These impedance spectra are consistent with the cycling performance of bare and fractional Al<sub>2</sub>O<sub>3</sub>-

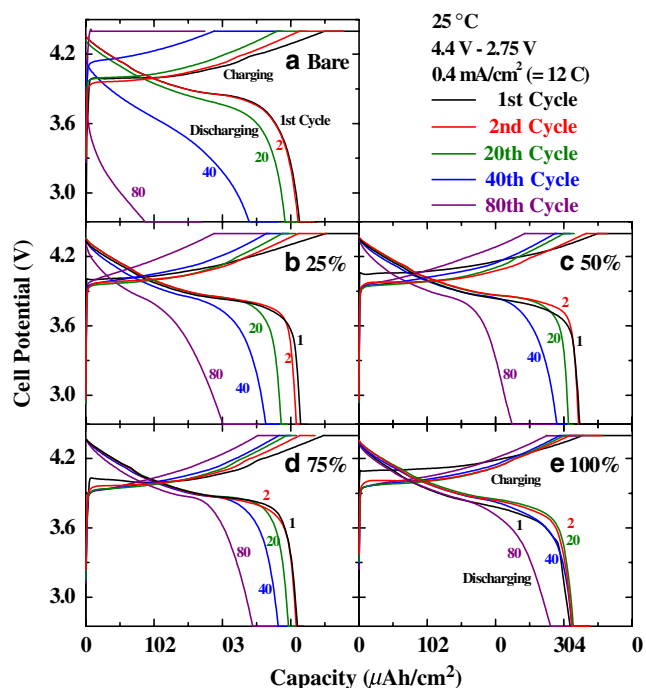


**Fig. 2** Voltage profiles of the **a** bare and Al<sub>2</sub>O<sub>3</sub>-coated LiCoO<sub>2</sub> films with **b** 25%, **c** 50%, **d** 75%, and **e** 100% surface coverage

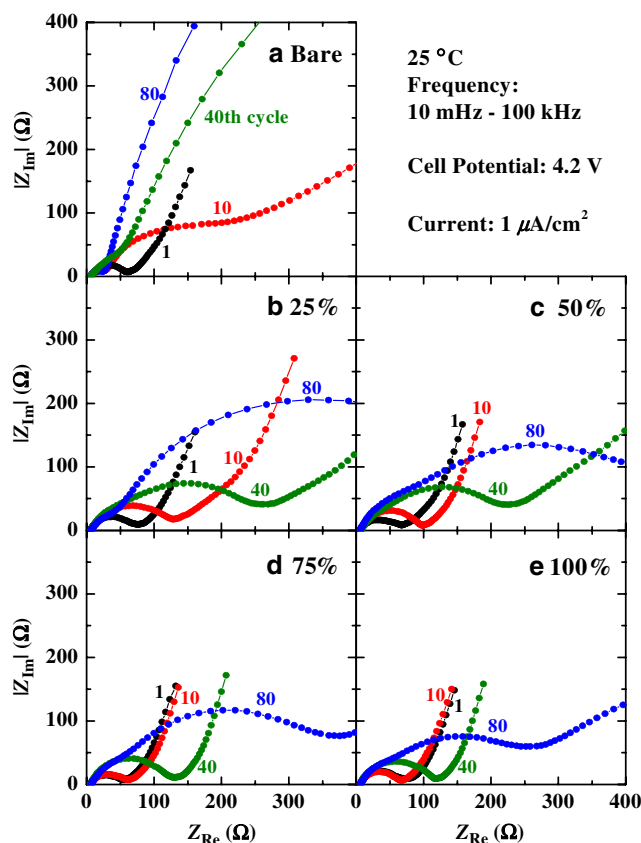


**Fig. 3** EIS of the **a** bare and Al<sub>2</sub>O<sub>3</sub>-coated LiCoO<sub>2</sub> films with **b** 25%, **c** 50%, **d** 75%, and **e** 100% surface coverage

coated LiCoO<sub>2</sub> films, because the increase in *R*<sub>ct</sub> is closely related to a deterioration of the electrochemical properties of the cathode during cycling.

The effect of Al<sub>2</sub>O<sub>3</sub>-coating coverage on the HF generation was examined by measuring the F<sup>-</sup> concentration in the electrolyte. The amount of F<sup>-</sup> decreases with increasing Al<sub>2</sub>O<sub>3</sub>-coating coverage. Moreover, the Al<sub>2</sub>O<sub>3</sub> coating with 100% coverage effectively inhibits F<sup>-</sup> generation (~300 ppm), which is much smaller than the F<sup>-</sup> concentration (~2,900 ppm) from the uncoated LiCoO<sub>2</sub> samples. It was reported that the decomposition of a LiPF<sub>6</sub>-based electrolyte with water leads to the formation of HF (LiPF<sub>6</sub>→LiF+PF<sub>5</sub> and PF<sub>5</sub>+H<sub>2</sub>O→POF<sub>3</sub>+2HF), which accompanies Co dissolution from LiCoO<sub>2</sub> [31, 32]. The amount of Co dissolution into the electrolyte from the uncoated LiCoO<sub>2</sub> thin film is ~460 ppm, while that from the Al<sub>2</sub>O<sub>3</sub>-coated LiCoO<sub>2</sub> film with 100% coverage is ~50 ppm, as shown in Fig. 4. There is a strong correlation between the amount of Co dissolution from the Al<sub>2</sub>O<sub>3</sub>-coated LiCoO<sub>2</sub> with different degrees of surface coverage and the charge-capacity retention after 100 cycles (shown in Fig. 1a). Although it is difficult to analyze the amount of scavenged water by the Al<sub>2</sub>O<sub>3</sub>-coating layer, the improved

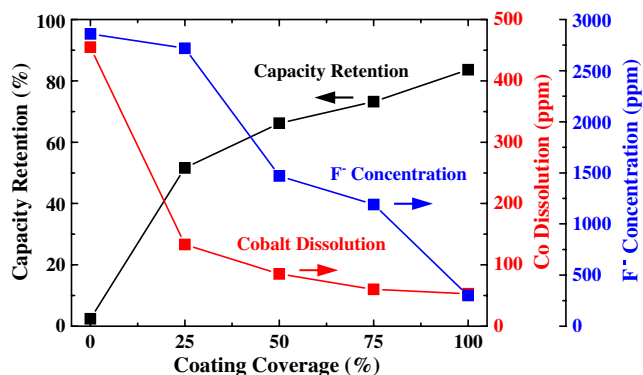


**Fig. 4** The charge-capacity retention after 100 cycles from Fig. 1a, and the Co dissolution and F<sup>-</sup> concentration in the electrolyte from bare and Al<sub>2</sub>O<sub>3</sub>-coated LiCoO<sub>2</sub> films with different coverage, after an initial 4.6 V charge and being immersed for 12 days at 25 °C

electrochemical properties even with partial coverage indicate an interaction between the coating layer and the electrolyte, which inhibits the HF generation by water scavenging.

Figure 5 shows the cycle-life performance of the bare and Al<sub>2</sub>O<sub>3</sub>-coated LiCoO<sub>2</sub> thin films with different coverage ratios at 60 °C. The Al<sub>2</sub>O<sub>3</sub>-coated LiCoO<sub>2</sub> films with 25% coverage show rapid capacity fading after ~70 cycles at 60 °C. However, the initial capacity and the capacity retention of the Al<sub>2</sub>O<sub>3</sub>-coated LiCoO<sub>2</sub> at 60 °C increase with the increasing Al<sub>2</sub>O<sub>3</sub>-coating coverage. The Al<sub>2</sub>O<sub>3</sub> coating with a coverage ranging from 50% to 100% shows excellent cycle-life performance at the elevated temperature.

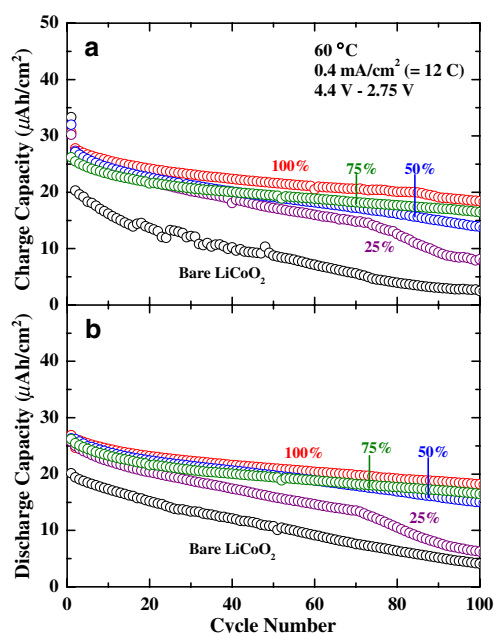


**Fig. 5** **a** The charge- and **b** discharge capacity retention of bare and Al<sub>2</sub>O<sub>3</sub>-coated LiCoO<sub>2</sub> films at 60 °C

The cycle-life performances of the bare and Al<sub>2</sub>O<sub>3</sub>-coated LiCoO<sub>2</sub> films with 200 ppm water-contaminated electrolytes at 25 °C were examined as a function of the surface coverage, as shown in Fig. 6. The initial capacity and the capacity retention with water impurities increase with the increasing Al<sub>2</sub>O<sub>3</sub>-coating coverage. The Al<sub>2</sub>O<sub>3</sub> coating even with partial coverage appears to inhibit the Co dissolution from acidic HF which occurs in the electrolyte.

In order to clarify the mechanisms of how an Al<sub>2</sub>O<sub>3</sub> coating effectively enhances the electrochemical properties of LiCoO<sub>2</sub> films under severe conditions, such as elevated temperature and additional water, the level of electrolyte decomposition was analyzed by measuring the amount of F<sup>-</sup> in the electrolyte. As shown in Fig. 7a, the F<sup>-</sup> concentration in the electrolyte of the Al<sub>2</sub>O<sub>3</sub>-coated LiCoO<sub>2</sub> with full coverage samples is extremely low compared with that of the bare samples. The Al<sub>2</sub>O<sub>3</sub> coating appears to suppress Co dissolution from LiCoO<sub>2</sub>, even at an elevated temperature and additional water impurity. This is correlated with the capacity retention of LiCoO<sub>2</sub> as a function of the coating coverage, as shown in Fig. 7b.

To investigate the reactions between the Al<sub>2</sub>O<sub>3</sub> coating and electrolyte with water contamination, the surface was examined by SIMS after 60 cycles in an electrolyte containing 200 ppm of water. In Fig. 8, the marked lines indicate the calculated ratios of mass/charge for AlO<sub>2</sub><sup>-</sup> (80.97 Th, Th=1 hydrogen atomic mass/electron charge), AlF<sub>4</sub><sup>-</sup> (102.98 Th) and CoOH<sup>+</sup> (75.94 Th), respectively. A fragment of CoOH<sup>+</sup>, which is attributed to cobalt dissolution

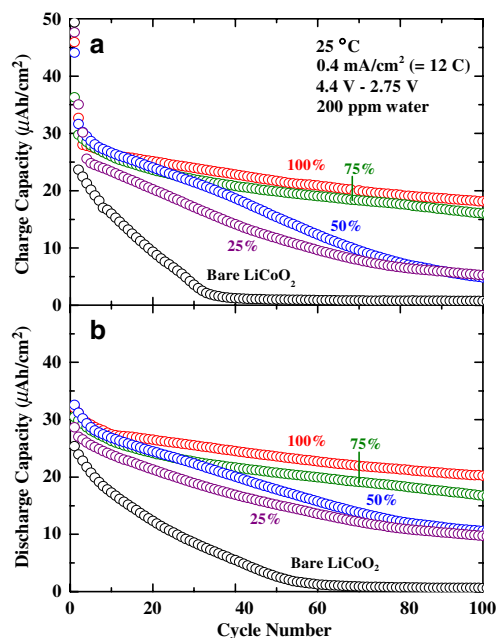


**Fig. 6** **a** The charge- and **b** discharge capacity retention of bare and Al<sub>2</sub>O<sub>3</sub>-coated LiCoO<sub>2</sub> films at 25 °C with 200 ppm water-contaminated electrolyte



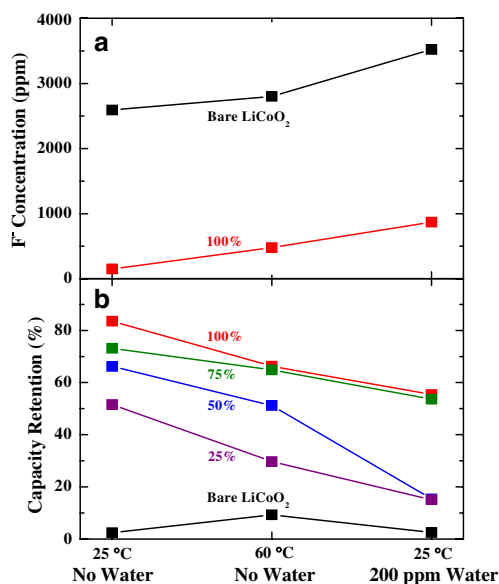


**Fig. 7** **a** The F<sup>-</sup> concentration in the electrolyte from bare and Al<sub>2</sub>O<sub>3</sub>-coated LiCoO<sub>2</sub> films with 100% coverage, after an initial 4.6 V charge and being immersed for 12 days at 25 °C, 60 °C, and 25 °C with 200 ppm water, respectively. **b** The charge-capacity retention of Al<sub>2</sub>O<sub>3</sub>-coated LiCoO<sub>2</sub> films, after 100 cycles at 25 °C (Fig. 1), 60 °C (Fig. 5), and 25 °C with 200 ppm water (Fig. 6)

tion from LiCoO<sub>2</sub> was observed on the surface of the bare LiCoO<sub>2</sub> films. However, the amount of CoOH<sup>+</sup> on the surface decreased significantly even with a 50% Al<sub>2</sub>O<sub>3</sub> coating, as shown in Fig. 8c.

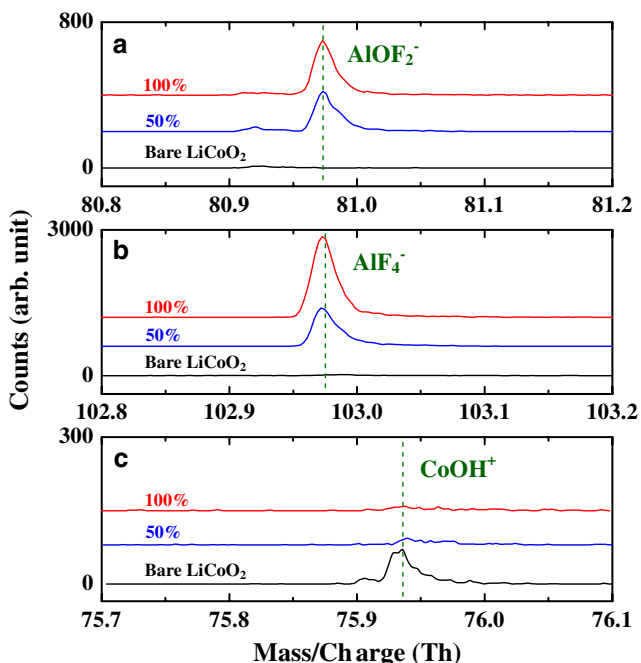


**Fig. 8** SIMS spectra of bare and Al<sub>2</sub>O<sub>3</sub>-coated LiCoO<sub>2</sub> thin films, after 60 cycles with 200 ppm of water impurities in the electrolyte

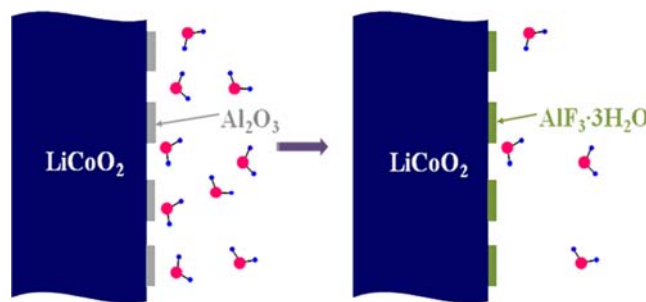


**Fig. 9** Schematic figure of H<sub>2</sub>O scavenging by Al<sub>2</sub>O<sub>3</sub>-coating layer

Kleist et al. reported that bulk Al<sub>2</sub>O<sub>3</sub> powders react with HF and H<sub>2</sub>O in an electrolyte to form AlF<sub>3</sub>·3H<sub>2</sub>O complexes at room temperature after 3 days [Al<sub>2</sub>O<sub>3</sub>+6HF+3H<sub>2</sub>O→2(AlF<sub>3</sub>·3H<sub>2</sub>O)], which was confirmed by the sharp X-ray diffraction peak widths [33]. Density-functional theory calculations also showed that AlF<sub>3</sub>·3H<sub>2</sub>O complexes were energetically favorable compared to AlF<sub>3</sub> and water, by ~2 eV/AlF<sub>3</sub> [34]. With these studies, the SIMS data of AlOF<sub>2</sub><sup>-</sup> and AlF<sub>4</sub><sup>-</sup> suggest that an Al<sub>2</sub>O<sub>3</sub>-coated layer scavenges H<sub>2</sub>O molecules, which improves the electrochemical properties of LiCoO<sub>2</sub> cathodes (Fig. 9).

**Conclusions**

This study examined the electrochemical properties of nanoscale Al<sub>2</sub>O<sub>3</sub>-coated LiCoO<sub>2</sub> thin films as a function of the coating coverage. These results were attributed to the suppression of Co dissolution and decomposition of LiPF<sub>6</sub> by extensive cycling. It was found that AlF<sub>3</sub>·3H<sub>2</sub>O was formed from the Al<sub>2</sub>O<sub>3</sub>-coating layer by a reaction with HF and H<sub>2</sub>O, thereby scavenging H<sub>2</sub>O molecules in the electrolyte and consequently decreasing the amount of HF. The enhanced electrochemical properties with various degrees of coating coverage were correlated with the affinity of metal fluoride to scavenge H<sub>2</sub>O impurities in the electrolyte. It still remains a question that how many H<sub>2</sub>O molecules can be scavenged by Al<sub>2</sub>O<sub>3</sub> coating, and what the effective partial-coating thickness is. In addition, direct evidence of AlF<sub>3</sub>·3H<sub>2</sub>O with reaction kinetics between Al<sub>2</sub>O<sub>3</sub> coating layer and HF/H<sub>2</sub>O also needs to be clarified experimentally.

**Acknowledgement** This work was supported by the National Research Foundation of Korea, through the Research Center for Energy Conversion and Storage (RCECS, R11-2002-102-00000-0) and the World Class University (WCU, R31-2008-000-10075-0).

## References

1. Tarascon JM, Armand M (2001) *Nature* 414:359
2. Wang H, Jang Y, Huang B, Sadoway DR, Chiang Y (1999) *J Electrochem Soc* 146:473
3. Amatucci GG, Tarascon JM, Klein LC (1996) *Solid State Ionics* 83:167
4. Venkatrman S, Manthiram A (2003) *Chem Mater* 15:5003
5. Aurbach D, Markovsky B, Rodkin A, Levi E, Cohen YS, Kim H, Schmidt M (2002) *Electrochim Acta* 47:4291
6. Jiang J, Buhrmester T, Eberman KW, Krause LJ, Dahn JR (2005) *J Electrochem Soc* 152:A19
7. Li D, Ito A, Kobayakawa K, Sato Y (2007) *Electrochim Acta* 52:1919
8. Cho J, Kim YJ, Kim T, Park B (2001) *Angew Chem Int Ed* 40:3367
9. Kim YJ, Lee E, Kim H, Cho J, Cho YW, Park B, Oh SM, Yoon JK (2004) *J Electrochem Soc* 151:A1063
10. Kim YJ, Kim H, Kim B, Ahn D, Lee J, Kim T, Son D, Cho J, Kim Y, Park B (2003) *Chem Mater* 15:1505
11. Cho J, Kim T, Kim C, Lee J, Kim Y, Park B (2005) *J Power Sources* 146:58
12. Kim YJ, Cho J, Kim T, Park B (2003) *J Electrochem Soc* 150:A1723
13. Chen Z, Dahn JR (2003) *Electrochem Solid-State Lett* 6:A221
14. Cho J, Kim Y, Kim B, Lee J, Park B (2003) *Angew Chem Int Ed* 42:1618
15. Kim B, Kim C, Ahn D, Moon T, Ahn J, Park Y, Park B (2007) *Electrochem Solid-State Lett* 10:A32
16. Ahn D, Kim C, Lee J, Kim B, Park Y, Park B (2007) *J Mater Res* 22:688
17. Li C, Zhang HP, Fu LJ, Liu H, Wu YP, Rahm E, Holze R, Wu HQ (2006) *Electrochim Acta* 51:3872
18. Cho J, Kim YJ, Park B (2001) *J Electrochem Soc* 148:A1110
19. Cho J, Kim YJ, Park B (2000) *Chem Mater* 12:3788
20. Kweon H, Park JJ, Seo JW, Kim GB, Jung BH, Lim HS (2004) *J Power Sources* 126:156
21. Liu L, Chen L, Huang X, Yang X, Yoon W, Lee HS, McBreen J (2004) *J Electrochem Soc* 151:A1344
22. Fey G, Yang HZ, Kumara T, Naik S, Chiang A, Lee DC, Lin JR (2004) *J Power Sources* 132:172
23. Thackeray MM, Johnson CS, Kim J, Lauzze KC, Vaughey JT, Dietz N, Abraham D, Hackney SA, Zeltner W, Anderson MA (2003) *Electrochem Comm* 5:752
24. Myung S, Izumi K, Komaba S, Sun Y, Yashiro H, Kumagai N (2005) *Chem Mater* 17:3695
25. Myung S, Izumi K, Komaba S, Yashiro H, Bang HJ, Sun Y, Kumagai N (2007) *J Phys Chem C* 111:4061
26. Van Landschoot N, Kelder EM, Kooyman PJ, Kwakernaak C, Schoonman J (2004) *J Power Sources* 138:262
27. Oh S, Lee JK, Byun D, Cho WI, Cho BW (2004) *J Power Sources* 132:249
28. Oh Y, Ahn D, Nam S, Kim C, Lee J, Park B (2008) *Electron Mater Lett* 4:103
29. Fey G, Chen J, Kumar TP (2005) *J Appl Electrochem* 35:177
30. Fey G, Kao HM, Muralidharan P, Kumar TP, Cho YD (2006) *J Power Sources* 163:135
31. Markovsky B, Rodkin A, Salitra G, Talyossef Y, Aurbach D, Kim H (2004) *J Electrochem Soc* 151:A1068
32. Edström K, Gustafsson T, Thomas JO (2004) *Electrochim Acta* 50:397
33. Kleist W, Haeßner C, Storcheva O, Köhler K (2006) *Inorg Chim Acta* 359:4851
34. Krossner M, Scholz G, Stösser R (1997) *J Phys Chem A* 101:1555